Neutrino Masses and Right-Handed Weak Currents Studied by Neutrino-Less $\beta\beta$-Decay Detectors

Saori Umehara *[ID] and Hiroyasu Ejiri [ID]

Research Center for Nuclear Physics, Osaka University, Osaka 567-0047, Japan; ejiri@rcnp.osaka-u.ac.jp
* Correspondence: umehara@rcnp.osaka-u.ac.jp

Abstract: Detecting neutrino-less double beta ($0\nu\beta\beta$) decay with high-sensitivity $0\nu\beta\beta$ detectors is of current interest for studying the Majorana neutrino's nature, the neutrino mass (ν-mass), right-handed weak currents (RHCs), and others beyond the Standard Model. Many experimental groups have studied $0\nu\beta\beta$ decay with ν-mass sensitivities on the order of 100 meV and RHC sensitivities on the order of 10^{-9}–10^{-6}, but no clear $0\nu\beta\beta$ signals have been observed so far in these ν-mass and RHC regions. Thus, several experimental groups are developing higher-sensitivity detectors to explore a smaller ν-mass region around 15–50 meV, which corresponds to the inverted hierarchy ν-mass, and smaller RHC regions on the order of 10^{-10}–10^{-7} in the near future. Nuclear matrix elements (NMEs) for ν-mass and RHC processes are crucial for extracting the ν-mass and RHCs of particle physics interest from $0\nu\beta\beta$ experiments. This report briefly reviews detector sensitivities and upper limits on the ν-mass and right-handed currents for several current $0\nu\beta\beta$ detectors and the ν-mass and RHC sensitivities expected for some near-future ones.

Keywords: neutrino-less double beta ($0\nu\beta\beta$) decay; $0\nu\beta\beta$ detector sensitivity; neutrino mass; right-handed weak current; present and future $0\nu\beta\beta$ detectors

1. Introduction

Neutrino-less double beta ($0\nu\beta\beta$) decay, which violates the lepton-number (L) conservation law by $\Delta L = 2$, is a sensitive and realistic probe for studying the neutrino's nature (Majorana or Dirac), the neutrino mass (ν-mass) and mass hierarchy, the neutrino CP phases, right-handed weak currents (RHCs), and others beyond the Standard Model (SM) [1–5].

$0\nu\beta\beta$ decay is a second-order weak process beyond the SM. Thus, the transition rate is on the order of 10^{-27}–10^{-30}/y, depending on the ν-mass and RHCs and also on their nuclear matrix elements (NMEs). The energy signal is only a few MeV, which is of the same order of magnitude as radioactive RI backgrounds. Accordingly, one needs large, ultra-low-background detectors to search for the neutrino's nature, the ν-mass, RHCs, and others.

$0\nu\beta\beta$-decay rate is proportional to the square of the nuclear matrix element NME ($|M^{0\nu}|$) [5–10]. Thus, an NME is crucial for extracting the effective ν-mass, RHCs, and other quantities of particle physics interest from the experimental $0\nu\beta\beta$-decay rates, once they are measured. An NME is also needed to design detectors for $0\nu\beta\beta$-decay measurements since the number of $\beta\beta$ isotopes required to measure the ν-mass is inversely proportional to the square of the NME. In fact, the backgrounds in the $0\nu\beta\beta$ signal region and NME greatly depend on $\beta\beta$ detectors and $\beta\beta$ nuclei to be used to search for the $0\nu\beta\beta$ signal. Accordingly, it is crucial to carry out high-sensitivity $\beta\beta$ experiments for several $\beta\beta$ isotopes with several types of $\beta\beta$ detectors. Recent $0\nu\beta\beta$ experiments and near-future plans are reviewed in [11,12], and theoretical and experimental studies of NMEs are given in reviews [5,13].

The present report aims to briefly review the current status and future prospects of $0\nu\beta\beta$ detectors in the search for the ν-mass and RHCs by measuring $\beta\beta$ decays on medium–heavy nuclei of current interest.

2. Neutrino Mass and RHC Sensitivities

The $0\nu\beta\beta$ rate, in the case of the left–right symmetric model, is conventionally given using the half-life $T_{1/2}^{0\nu}$, as shown in review articles and references therein [1–7]. It is noted that high-sensitivity $\beta\beta$ detectors are very powerful in exploring possible RHCs beyond the SM as well as the ν-mass in the framework of the left–right symmetric models [1–7]. The rate is given as

$$
\begin{aligned}
\frac{1}{T_{1/2}^{0\nu}} \;=\; & C_{mm}\left(\frac{\langle m_{0\nu}\rangle}{m_e}\right)^2 + C_{\lambda\lambda}\langle\lambda\rangle^2 + C_{\eta\eta}\langle\eta\rangle^2 \\
& + C_{m\lambda}\frac{\langle m_{0\nu}\rangle}{m_e}\langle\lambda\rangle + C_{m\eta}\frac{\langle m_{0\nu}\rangle}{m_e}\langle\eta\rangle + C_{\lambda\eta}\langle\lambda\rangle\langle\eta\rangle,
\end{aligned}
\tag{1}
$$

where $\langle m_{0\nu}\rangle$, $\langle\lambda\rangle$, and $\langle\eta\rangle$ are the effective ν-mass, the effective λ-RHC, and the effective η-RHC, respectively. The right-handed $\langle\lambda\rangle$ and $\langle\eta\rangle$ terms are expressed in terms of the square of the mass ratio of the left-handed weak boson to the right-handed weak boson and their mixing angle, respectively. The C coefficient of C_{ij}, with i and j being $\langle m_{0\nu}\rangle$, $\langle\lambda\rangle$ and $\langle\eta\rangle$, is expressed by the product of the phase-space factor and the NME. In the case of the light ν-mass process, $T_{1/2}^{0\nu}$ is expressed as [1,4,6]

$$
\frac{1}{T_{1/2}^{0\nu}} \;=\; g_A^4 \cdot G_{01}^{0\nu} \cdot |M_m^{0\nu}|^2 \cdot \left(\frac{\langle m_{0\nu}\rangle}{m_e}\right)^2,
\tag{2}
$$

where $g_A = 1.27$ is the weak axial-vector coupling for a free nucleon in units of the weak vector coupling, $G_{01}^{0\nu}$ is the phase-space factor, $|M_m^{0\nu}|$ is the NME for the light ν-mass process, and m_e is the electron mass. Here, the quenching effect on the weak coupling of g_A is included in the NME since the effect is due to nuclear effects, as discussed later. One experimentally obtains

$$
\frac{1}{T_{1/2}^{0\nu} \cdot g_A^4 \cdot G_{01}^{0\nu}} = \left(|M_m^{0\nu}| \cdot \left(\frac{\langle m_{0\nu}\rangle}{m_e}\right)\right)^2,
\tag{3}
$$

i.e., the square of the product of $|M_m^{0\nu}|$ and $\langle m_{0\nu}\rangle$. Here, the left-hand side is the value to be measured, and the right-hand one is the value of nuclear particle physics interest.

In the case of λ-RHC $0\nu\beta\beta$ decay, the rate is approximately expressed as [1,4,6]

$$
\begin{aligned}
\frac{1}{T_{1/2}^{0\nu}} &\;=\; g_A^4 \cdot G_{02}^{0\nu} \cdot |M_\lambda^{0\nu}|^2 \cdot \langle\lambda\rangle^2, \\
|M_\lambda^{0\nu}| &\;=\; |M_{\mathrm{GT}}^{0\nu}||\chi_{2-}(1+\epsilon_\lambda)|,
\end{aligned}
\tag{4}
$$

where $G_{02}^{0\nu}$ is the phase-space factor [14], $|M_{\mathrm{GT}}^{0\nu}|$ is the Gamow–Teller NME for the ν-mass term, χ_{2-} is the λ-NME, and ϵ_λ is for the contributions from other terms. The value for ϵ_λ is around 10–30%, depending on the individual nucleus.

In the case of the η-RHC $0\nu\beta\beta$, the rate is approximately expressed as [1,4,6]

$$
\begin{aligned}
\frac{1}{T_{1/2}^{0\nu}} &\;=\; g_A^4 \cdot G_{09}^{0\nu} \cdot |M_\eta^{0\nu}|^2 \cdot \langle\eta\rangle^2, \\
|M_\eta^{0\nu}| &\;=\; |M_{\mathrm{GT}}^{0\nu}||\chi_R|,
\end{aligned}
\tag{5}
$$

where $G_{09}^{0\nu}$ is the phase-space factor [14], and χ_R is the η-NME. Here, we consider the main term with the phase-space factor of $G_{09}^{0\nu}$ since the other terms are around 2 orders of magnitudes smaller than the main term.

The mass sensitivity, $\langle m_{0\nu} \rangle^s$, is defined as the minimum effective ν-mass to be measured experimentally [5,13]. Then, in the case of the current non-zero-background experiments, the minimum $|M_m^{0\nu}|\langle m_{0\nu} \rangle$ to be studied is expressed as

$$
\begin{aligned}
|M_m^{0\nu}|\langle m_{0\nu} \rangle^s &= k_m \cdot \sqrt{\frac{UL(B)}{N \cdot T}} \cdot \sqrt{\frac{A}{g_A^4 \cdot G_{01}^{0\nu}}}, \\
k_m &= m_e \cdot 1.5 \times 10^{-8} \\
&= 7.8 \text{ meV}
\end{aligned}
\tag{6}
$$

where $UL(B)$ is the upper limit for $0\nu\beta\beta$ events in the region of interest (ROI). N is the total mass of the $\beta\beta$ isotopes in units of tons, and T is the exposure time in units of years. A is the mass number of the $\beta\beta$ nucleus. $G_{01}^{0\nu}$ is in units of 10^{-14}, as shown in Table 1. Here, we assumed for simplicity that the detector efficiency is 1. When the background rate $(B \cdot N \cdot T)$ statistics follow a Gaussian distribution, $UL(B)$ is given as $\sqrt{B \cdot N \cdot T}$, where B is the background rate (/ton·year) in the ROI. On the other hand, in "background-free measurement", the background rate statistics do not follow a Gaussian distribution, and $UL(B)$ is proportional to $N \cdot T$ due to the properties of the Poisson distribution. All future experiments given here are not "background-free measurement" but aim at background rates of $B \simeq 1$, which is called "quasi-background-free measurement" in [12], i.e., backgrounds around 10 in the case of a 2 ton $\times$ 5 years run.

Table 1. Phase-space factors $G_{01}^{0\nu}, G_{02}^{0\nu}$, and $G_{09}^{0\nu}$ in units of yr^{-1}. As shown in table 1 in [15], the s-wave electron phase-space factors (PSFs) ($G_{01}^{0\nu}$) are from [16], and the p-wave electron PSFs ($G_{02}^{0\nu}$ and $G_{09}^{0\nu}$) are from [14].

	^{48}Ca	^{76}Ge	^{82}Se	^{96}Zr	^{100}Mo	^{116}Cd	^{130}Te	^{136}Xe	^{150}Nd
$G_{01}^{0\nu} \cdot 10^{14}$	2.465	0.2372	1.014	2.048	1.584	1.662	1.424	1.454	6.194
$G_{02}^{0\nu} \cdot 10^{14}$	16.229	0.391	3.529	8.959	5.787	5.349	3.761	3.679	29.187
$G_{09}^{0\nu} \cdot 10^{10}$	16.246	1.223	4.779	8.619	6.540	6.243	4.972	4.956	19.454

Here, $\sqrt{UL(B)/(N \cdot T)}$ stands for the detector sensitivity, and $g_A^4 \cdot G_{01}^{0\nu}$ for the atomic one. In real $\beta\beta$ experiments, backgrounds are on the order of 10 or so, the signal rate depends on the detector and analysis efficiencies, and the limits are evaluated at the 90% confidence level. The sensitivities in these real cases are discussed in [12]. The ν-mass sensitivity in real experiments is discussed in terms of the nuclear sensitivity and the detector sensitivity with the efficiency ϵ in [12].

Similarly, the RHC sensitivities are given by $G_{02}^{0\nu}$ in units of 10^{-14} and $G_{09}^{0\nu}$ in units of 10^{-14} as

$$
\begin{aligned}
|M_\lambda^{0\nu}|\langle \lambda \rangle^s &= k_\lambda \cdot \sqrt{\frac{UL(B)}{N \cdot T}} \cdot \sqrt{\frac{A}{g_A^4 \cdot G_{02}^{0\nu}}}, \\
k_\lambda &= 1.5 \times 10^{-8}
\end{aligned}
\tag{7}
$$

$$
\begin{aligned}
|M_\eta^{0\nu}|\langle \eta \rangle^s &= k_\eta \cdot \sqrt{\frac{UL(B)}{N \cdot T}} \cdot \sqrt{\frac{A}{g_A^4 \cdot G_{09}^{0\nu}}}, \\
k_\eta &= 1.5 \times 10^{-8}
\end{aligned}
\tag{8}
$$

In the case of a large background rate of $B \cdot N \cdot T \gg 1$, the coefficient of $\sqrt{UL(B)/(N \cdot T)}$ is rewritten as $\sqrt[4]{B/(N \cdot T)}$, because the background fluctuations adopt a Gaussian distribution. Thus, the minimum ν-mass $\langle m_{0\nu} \rangle$ and the minimum RHCs of $\langle \lambda \rangle$ and $\langle \eta \rangle$ to be measured are inversely proportional to NMEs and $\sqrt[4]{N \cdot T}$. They are very sensitive to NMEs, but not to N and T. In other words, one is forced to require 5 times more $\beta\beta$ isotopes or 5 times longer run time if the NME is 32% smaller.

3. Sensitivities of Current and Near-Future $\beta\beta$ Detectors

Many high-sensitivity $0\nu\beta\beta$ experiments have been carried out so far and/or are being run using higher-sensitivity $0\nu\beta\beta$ detectors. Many experimental groups are developing higher-sensitivity $0\nu\beta\beta$ detectors. Some of them plan to build ton-scale detectors to study $0\nu\beta\beta$ in the half-life region on the order of 10^{27} y.

Figure 1 shows the current experimental results and proposed projects' sensitivities for $|M_m^{0\nu}|\langle m_{0\nu}\rangle^s$. The figure shows the sensitivities of CANDLES (^{48}Ca) [17], GERDA-II (^{76}Ge) [18], CUPID-0 (^{82}Se) [19], NEMO-3 (^{96}Zr) [20], CUPID-Mo (^{100}Mo) [21], Aurora (^{116}Cd) [22], CUORE (^{130}Te) [23], KamLAND-Zen (^{136}Xe) [24], and NEMO-3 (^{150}Nd) [25], which have a status of data taking/completed. In addition, we list the sensitivities of LEGEND-1000 (^{76}Ge) [26], SuperNEMO (^{82}Se) [27], CUPID (^{100}Mo) [28], SNO+II (^{130}Te) [29], and nEXO (^{136}Xe) [30] for proposed projects for each nucleus. Here, the half-life sensitivities for future projects are the values given in table IV of [12]. Although many $0\nu\beta\beta$ decay experiments, such as MAJORANA (^{76}Ge) [31], AMoRE (^{100}Mo) [32], KamLAND2-Zen (^{136}Xe) [33], EXO-200 (^{136}Xe) [34], NEXT (^{136}Xe) [35], PandaX-III-200 (^{136}Xe) [36], LZ (^{136}Xe) [37], DARWIN (^{136}Xe) [38], and others, have been carried out and are proposed for future projects, here, we list one experiment for each nucleus for reference.
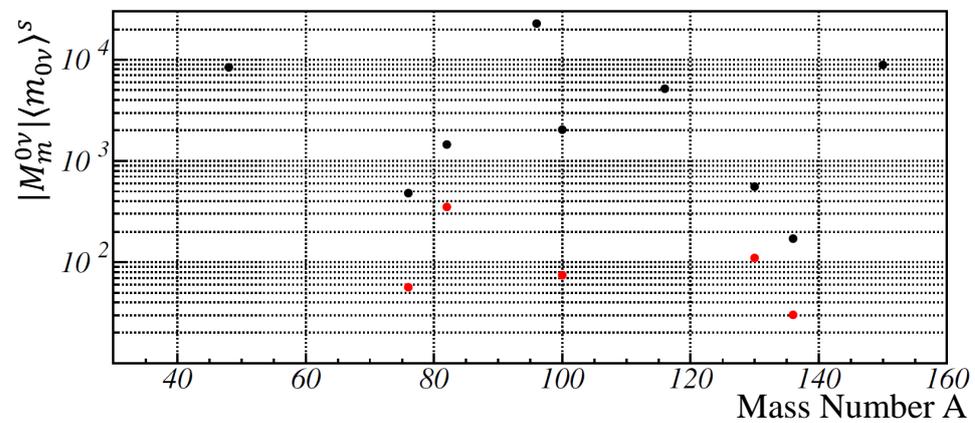
Figure 1. Sensitivities for current experiments and proposed projects. Black dots are for current experiments and red dots are for proposed projects. The plotted points show the sensitivity $|M_m^{0\nu}|\langle m_{0\nu}\rangle^s$ in units of meV.

In the present report, we mainly discuss calorimetric $0\nu\beta\beta$ detectors for future projects with high discovery potential. Accordingly, the angular and energy correlations of the two β rays from $0\nu\beta\beta$ events are not measured. Then, it is hard to identify individual ν-mass and RHC processes involved in $0\nu\beta\beta$ events.

$0\nu\beta\beta$ detectors such as ELEGANT V [39], MOON [40,41], NEMO-III [42], and Super NEMO [43] measure individual $\beta\beta$ tracks as well as their energies and thus are useful in verifying $\beta\beta$ events and identifying the processes, mass, λ, and/or η processes once $0\nu\beta\beta$ events are observed by calorimetric detectors. Other projects are described in detail in reference [12].

The $0\nu\beta\beta$ decays to be discussed are mainly double β^- decays of ground-state to ground-state transitions of $_Z^A X \rightarrow_{Z+2}^A X$, with A and Z being the mass and proton number, for medium–heavy nuclei with high sensitivity [13]. We note that $|M_m^{0\nu}|$ is more or less close to $|M_\lambda^{0\nu}|$ and $|M_\eta^{0\nu}|$ in pnQRPA model calculations. In this case, the ν-mass sensitivity in units of m_e and the $\langle\lambda\rangle$ and $\langle\eta\rangle$ sensitivities are proportional to the square roots of the phase-space factors $\sqrt{G_{01}^{0\nu}}$, $\sqrt{G_{02}^{0\nu}}$ and $\sqrt{G_{09}^{0\nu}}$. As shown in Table 1, the value for the phase-space factor of $G_{02}^{0\nu}$ is larger than that for $G_{01}^{0\nu}$ by a factor of 3–6, and thus, the $\langle\lambda\rangle^s$ sensitivity is higher (smaller) than the mass sensitivity by a factor of around 2, while the value for $G_{09}^{0\nu}$ is larger than that for $G_{02}^{0\nu}$ by 4 orders of magnitude, and thus, the $\langle\eta\rangle^s$ sensitivity is higher than the $\langle\lambda\rangle^s$ sensitivity by 2 orders of magnitude. In other words, high-sensitivity

$\beta\beta$ detectors with an $\langle m_{0\nu}\rangle^s$ sensitivity of 10^{-7} (i.e., 50 meV) are used to search for the RHCs of $\langle\lambda\rangle^s$ and $\langle\eta\rangle^s$ in the regions of 5×10^{-8} and 5×10^{-10}, respectively.

The current limits and the proposed projects' sensitivities $|M_\lambda^{0\nu}|\langle\lambda\rangle^s$ and $|M_\eta^{0\nu}|\langle\eta\rangle^s$ are shown in Figures 2 and 3.
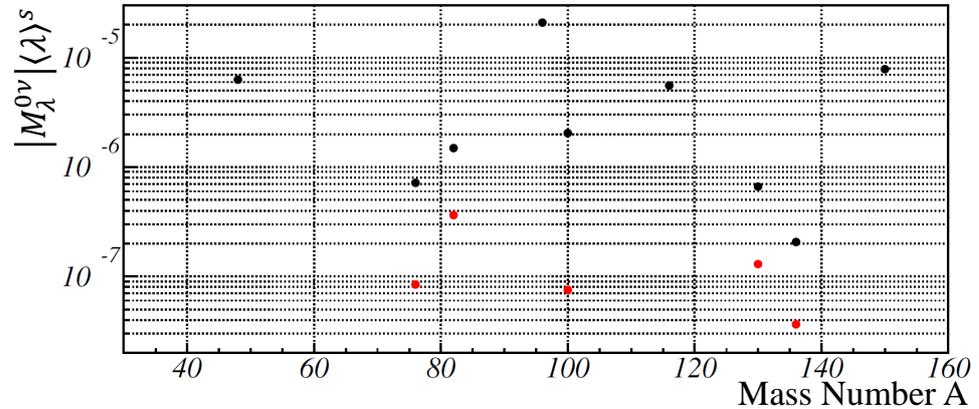
Figure 2. Sensitivities for current experiments and proposed projects. See the Figure 1 caption. The plots are shown for the sensitivity $|M_\lambda^{0\nu}|\langle\lambda\rangle^s$.
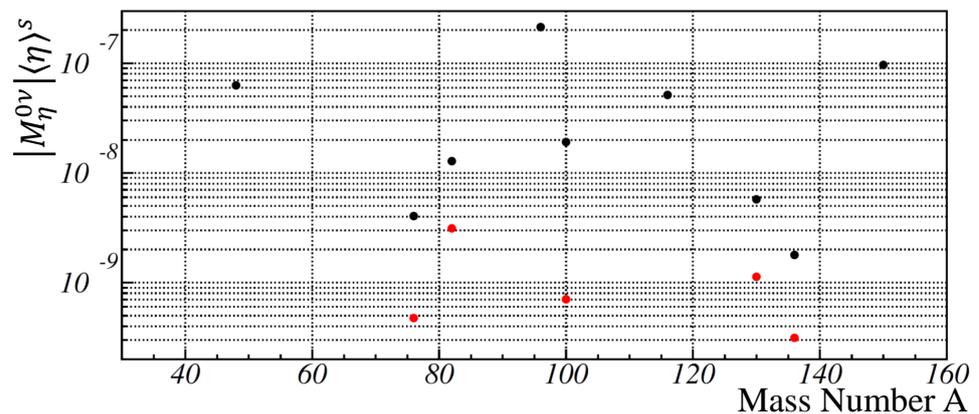
Figure 3. Sensitivities for current experiments and proposed projects. See the Figure 1 caption. The plots are shown for the sensitivity $|M_\eta^{0\nu}|\langle\eta\rangle^s$.

4. $\beta\beta$ Sensitivities and NMEs

The ν-mass and RHC sensitivities defined in Equations (6)–(8) include their NMEs for $\beta\beta$ nuclei. Actually, the values of the effective ν-mass and RHCs are inversely proportional to their NMEs of $|M_m^{0\nu}|$, $|M_\lambda^{0\nu}|$, and $|M_\eta^{0\nu}|$, which reflect the nuclear structures involved in the ν-mass and RHC processes. Then, NMEs are indispensable for deriving the ν-mass and the RHCs of particle physics interest from the $\beta\beta$ rates, once observed, and for designing $\beta\beta$ detectors to search for the effective ν-mass and RHCs in the given regions.

As shown in Figures 1–3, the most sensitive measurement in the proposed projects is in the experiment using ^{136}Xe. This is because ^{136}Xe is easily enriched, and thus, large numbers of $\beta\beta$ decay nuclei can be used. ^{130}Te can realize the high-sensitivity measurement as well because ^{130}Te has a high natural isotope ratio, which makes it possible to use a large number of $\beta\beta$ decay nuclei. The merit of ^{76}Ge is the high energy resolution, which is important for low-background measurements. These current high-sensitivity experiments have used 0.5–5 kmol $\beta\beta$ decay nuclei, and in future experiments, $\sim$50 kmol $\beta\beta$ decay nuclei will be used. For ^{100}Mo, future projects using 1–2 kmol $\beta\beta$ decay nuclei are proposed. ^{100}Mo has good nuclear sensitivity, and thus, the measurement sensitivity is relatively good for the number of $\beta\beta$ decay nuclei. ^{48}Ca, ^{96}Zr, and ^{150}Nd have larger phase-space factors. However, unfortunately, large-scale isotope separation systems have not yet been constructed. When the system is constructed, it will be possible to make highly sensitive

$\beta\beta$ decay measurements with a relatively small number of $\beta\beta$ nuclei if their NMEs are not much smaller than those for others.

Recently, a $0\nu\beta\beta$ experiment for the ν-mass process was extensively discussed because the effective mass is expected to be a finite value of around 15–50 meV in the case of an inverted mass hierarchy, depending on the phase. This is the region to be studied by future ton-scale detectors. The effective mass decreases below around 5 meV in the case of the normal mass hierarchy. The NME $|M_m^{0\nu}|$ for the ν-mass process has been evaluated using various kinds of nuclear models. The $0\nu\beta\beta$-NME for the light ν-mass process is given as [5]

$$|M_m^{0\nu}| = \left(\frac{g_A^{\text{eff}}}{g_A}\right)^2 \cdot [M_{\text{GT}}^{0\nu} + M_{\text{T}}^{0\nu}] + \left(\frac{g_V^{\text{eff}}}{g_A}\right)^2 \cdot M_{\text{F}}^{0\nu}, \tag{9}$$

where $M_{\text{GT}}^{0\nu}$, $M_{\text{T}}^{0\nu}$, and $M_{\text{F}}^{0\nu}$ are the axial-vector (GT: Gamow–Teller), tensor (T), and vector (F: Fermi) $\beta\beta$-NMEs, respectively, and g_A^{eff} and g_V^{eff} are introduced to incorporate quenching effects [44–48].

The $\beta\beta$ transitions are axial-vector spin–isospin ($\sigma\tau$) and vector isospin (τ) transitions. Thus, the NMEs greatly depend on nucleonic and non-nucleonic $\sigma\tau$ and τ interactions and their correlations. The proton-neutron Quasi-particle Random Phase Approximation (pnQRPA) model, which explicitly includes the nucleonic $\sigma\tau$ and τ interactions and their correlations, is widely used for $0\nu\beta\beta$-NME calculations. Then, NMEs $M_\alpha^{0\nu}$ with $\alpha = $ GT, T, F are given by the pnQRPA model NMEs, and then g_A^{eff}/g_A and g_V^{eff}/g_A represent effects due to such non-nucleonic $\sigma\tau$ and τ correlations and nuclear medium effects that are not explicitly included in the pnQRPA model [5].

The NMEs for RHC processes are also expressed as NMEs for light ν-mass processes in terms of the axial-vector and vector NMEs with nuclear spin–isospin and multipole operators. Thus, they are very sensitive to nucleonic and non-nucleonic $\sigma\tau$ and τ correlations and nuclear medium effects. Then, one has to use the effective weak couplings of g_A^{eff} and g_V^{eff} to incorporate such spin–isospin effects, which are not explicitly included in the model calculations [5].

So far, many theoretical calculations for $\beta\beta$-NMEs have been made using various kinds of theoretical models, as discussed in review articles and references therein [5–10]. The models are pnQRPA, ISM (Interacting Shell Model), IBM-2 (Interacting Boson Model), and others. In fact, the calculated NMEs greatly depend on the theoretical models and the nuclear parameters used in the models. Accordingly, the calculated values for $|M_m^{0\nu}|$ scatter over a region of an order of magnitude, depending on the models and the parameters. Among them, the critical nuclear parameters are the effective axial weak coupling of g_A^{eff}. Note the GT NME $|M_{\text{GT}}^{0\nu}|$ in Equation (9) with $(g_A^{\text{eff}})^2$ is the major component in the NME $|M_m^{0\nu}|$. The accurate evaluation of g_A^{eff} is extremely hard since it stands for non-nucleonic (mesons, isobars, etc.) effects and nuclear medium effects, which are hard to calculate accurately in most nuclear models based on nucleons only. In particular, the Δ isobar effect is very important for the GT and $\sigma\tau$ components of the NME. This effect is known to quench many single axial-vector NMEs and thus is considered to do so for the axial-vector components of $|M_m^{0\nu}|$, $|M_\lambda^{0\nu}|$, and $|M_\eta^{0\nu}|$.

There are no direct experimental methods for measuring $0\nu\beta\beta$-NMEs. On the other hand, several experimental inputs are effective in performing theoretical calculations for $\beta\beta$-NMEs.

Recently, single β decay, single charge-exchange reactions (CERs), and ordinary muon capture (OMC) reactions have been extensively studied to provide $\beta\beta$ theory models with useful NMEs associated with $\beta\beta$-NMEs, as discussed in [5,11,13]. The GT and SD (spin dipole) NMEs for single β decays of $_Z^A\text{X} \to _{Z+1}^A\text{X}$ and $_{Z+1}^A\text{X} \to _{Z+2}^A\text{X}$ have been used to obtain the NMEs associated with the $\beta\beta$-NME $_Z^A\text{X} \leftarrow _{Z+2}^A\text{X}$ via the intermediate state in $_{Z+1}^A\text{X}$. The (^{3}He, t) CER with medium-energy ^{3}He from the RCNP cyclotron has been extensively used to obtain the single GT and SD NMEs associated with the $\beta\beta$-NMEs for

medium–heavy nuclei. The OMC of $^A_{Z+2}X + \mu^- \to {}^A_{Z+1}X$ has been well studied using the μ-beam at RCNP to measure the NMEs associated with $\beta\beta$ via the intermediate nucleus $^A_{Z+1}X$. These experimental axial-vector NMEs are shown to be quenched with respect to the pnQRPA model NMEs by a factor of around $g_A^{\text{eff}}/g_A \sim 0.6$ [5,13]. The double-charge-exchange reaction (DCER) is of potential interest for studying $0\nu\beta\beta$-NMEs, as discussed in [49]. DCERs are studied using heavy-ion projectiles, and thus, they include various reaction processes and various nuclear interactions and are also sensitive to distortions of the projectile and the ejectile. Extensive DCER programs are ongoing, as given in [49].

Recently, NMEs for the light ν-mass process have been well studied by fully using the experimental NMEs for single β decays, single CERs, and OMCs, as well as theoretical pnQRPA NMEs [50]. They are shown to be given by a smooth function of the mass number A as $|M_m^{0\nu}| = 5.2 - 0.023A$ for medium–heavy nuclei of $A = 76$–136 [50].

The RHC-NMEs evaluated by QRPA model calculations are not much different from the ν-mass NME evaluated by the same QRPA model calculations [6]. Then, RHC-NMEs are considered to be given by a similar expression as a function of A. Then, using the simple expression $|M_m^{0\nu}| \approx |M_\lambda^{0\nu}| \approx |M_\eta^{0\nu}| \approx 5.2 - 0.023A$, one obtains $\beta\beta$-NMEs of 3.5, 3, and 2 for $\beta\beta$ nuclei with A of around 80, 100, and 130. Then, the $0\nu\beta\beta$ detector sensitivities for the ν-mass and RHCs are not sensitive to A. Thus, the selection of $0\nu\beta\beta$ nuclei to be used among medium–heavy nuclei may be made on the basis of experimental requirements such as ton-scale $0\nu\beta\beta$ isotopes, a large $G^{0\nu}$ (large $Q_{\beta\beta}$) value, low background, and high energy resolution.

The ν-mass and RHCs to be studied by near-future $\beta\beta$ detectors are evaluated using NMEs $\approx 5.2 - 0.023A$. The effective ν-masses are around 15, 100, 25, 50, and 15, all in units of meV, in the cases of the ^{76}Ge, ^{82}Se, ^{100}Mo, ^{130}Te, and ^{136}Xe experiments, respectively. Thus, the inverted mass hierarchy mass region will be well studied with near-future $\beta\beta$ detectors. The effective RHCs to be studied are around 1, 10, 3, 5, and 1, all in units of 10^{-8} for $\langle\lambda\rangle$ and 10^{-10} for $\langle\eta\rangle$, in the cases of the ^{76}Ge, ^{82}Se, ^{100}Mo, ^{130}Te, and ^{136}Xe experiments, respectively.

5. Summary and Concluding Remarks

The present report briefly reviews the $0\nu\beta\beta$ sensitivities in recent experiments and near-future plans for typical $0\nu\beta\beta$ nuclei on the basis of the left–right symmetric model. The sensitivities discussed are the ν-mass sensitivity $|M_m^{0\nu}|\langle m_{0\nu}\rangle^s$ and the RHC sensitivities $|M_\lambda^{0\nu}|\langle\lambda\rangle^s$ and $|M_\eta^{0\nu}|\langle\eta\rangle^s$, where $|M_m^{0\nu}|$, $|M_\lambda^{0\nu}|$, and $|M_\eta^{0\nu}|$ are the NMEs for the light ν-mass process and the RHC λ and η processes, respectively. The sensitivities in recent experiments are based on the reported half-life limits, and those for planned experiments are evaluated using the phase-space factors, the estimated background, and the total number of $\beta\beta$ isotopes.

Near-future ton-scale projects on $0\nu\beta\beta$ are all encouraged to explore new regions of ν-masses and weak RHCs. Experimental studies on several $\beta\beta$ nuclei are crucial since the NMEs and backgrounds depend on the nuclei and the detectors to be used. Among them, for future $0\nu\beta\beta$ detectors with ^{76}Ge, ^{100}Mo, ^{130}Te, and ^{136}Xe, it will be interesting to study the regions around $\langle m_{0\nu}\rangle = 10 - 55$ meV, $\langle\lambda\rangle = 1.2 \times 10^{-8} - 0.7 \times 10^{-7}$, and $\langle\eta\rangle = 1.0 \times 10^{-10} - 0.6 \times 10^{-9}$ by assuming 2–3 for $|M_m^{0\nu}|$, $|M_\lambda^{0\nu}|$, and $|M_\eta^{0\nu}|$. The NMEs for the ν-mass and RHC processes are crucial for extracting the effective ν-mass and the effective RHCs of particle physics interest beyond the SM. They are calculated using various theoretical models but are actually very sensitive to the nuclear models and nuclear parameters used in the models. Thus, experimental studies using single β decays, CERs, and OMCs are very valuable in helping theories evaluate reliable $0\nu\beta\beta$-NMEs.

It is noted that the $0\nu\beta\beta$ signal yield (the number of counts) is considered to be so small, depending on the ν-mass and the RHCs, that one has to know if it is NOT an unknown background γ peak or a quasi-peak due to a fluctuation in the background that happens to be located in the ROI of the $Q_{\beta\beta}$ value. Accordingly, it is crucial to observe similar $0\nu\beta\beta$ peaks in different ROIs for several $\beta\beta$ nuclei.

Here, we have exclusively discussed $0\nu\beta\beta$ to the 0^+ ground state, but $\beta\beta$ to the 2^+ excited state is of interest for studying the RHC $\langle\lambda\rangle$ process in the case where the 2^+ state is located in the relatively low-excitation region. $0\nu\beta\beta$ experiments for the excited 2^+ state will be discussed separately elsewhere.

Finally, we thank Prof. S. Stoica for great contributions to the progress of $\beta\beta$ nuclear physics.

References

1. Doi, M.; Kotani, T.; Takasugi, E. Double beta decays and Majorana Neutrino. *Prog. Theor. Phys. Suppl.* **1985**, *83*, 1–175. [CrossRef]
2. Haxton, W.C.; Stephenson, G.J., Jr. Double beta decay. *Prog. Part. Nucl. Phys.* **1984**, *12*, 409–479. [CrossRef]
3. Avignone, F.; Elliott, S.; Engel, J. Double beta decay, Majorana neutrino, and neutrino mass. *Rev. Mod. Phys.* **2008**, *80*, 481. [CrossRef]
4. Vergados, J.; Ejiri, H.; Šimkovic, F. Theory of neutrinoless double-β-decay. *Rep. Prog. Phys.* **2012**, *75*, 106301. [CrossRef] [PubMed]
5. Ejiri, H.; Suhonen, J.; Zuber, K. Neutrino nuclear responses for astro-neutrinos, single β-decays, and double β-decays. *Phys. Rep.* **2019**, *797*, 1–102. [CrossRef]
6. Suhonen, J.; Civitarese, O. Weak interaction and nuclear structure aspect of nuclear double beta decay. *Phys. Rep.* **1998**, *300*, 123–214. [CrossRef]
7. Faessler, A.; Simkovic, F. Double beta decay. *J. Phys. G Nucl. Part. Phys.* **1998**, *24*, 2139. [CrossRef]
8. Suhonen, J.; Civitarese, O. Double-beta decay nuclear matrix elements in the pnQRPA framework. *J. Phys. G Nucl. Part Phys.* **2012**, *39*, 035105. [CrossRef]
9. Barea, J.; Korita, J.; Iachello, F. Nuclear matrix elements for double-β decay. *Phys. Rev. C* **2013**, *87*, 014315. [CrossRef]
10. Engel, J.; Menéndez, J. Status and future of nuclear matrix elements for neutrinoless double β-decay: A review. *Rep. Prog. Phys.* **2017**, *60*, 046301. [CrossRef]
11. Detwiler, J. Future neutrinoless double-beta decay experiments. In Proceedings of the International Conference "Neutrino 2020", Chicago, IL, USA, 22 June–2 July 2020.
12. Agostini, M.; Benato, G.; Detwiler, J.A.; Menéndez, J.; Vissani, F. Toward the discovery of matter creation with neutrinoless $\beta\beta$ decay. *Rev. Mod. Phys.* **2023**, *95*, 025002. [CrossRef]
13. Ejiri, H. Experimental approaches to neutrino nuclear responses for $\beta\beta$-decays and astro-neutrins. *Front. Phys.* **2021**, *9*, 650421. [CrossRef]
14. Štefánik, D.; Dvornický, R.; Šimkovic, F.; Vogel, P. Reexamining the light neutrino exchange machanism of the $0\nu\beta\beta$ decay with left- and right-handed leptonic and hadronic currents. *Phys. Rev. C* **2015**, *92*, 055502. [CrossRef]
15. Neacsu, A.; Sevestrean, V.A.; Stoica, S. Brief Review of the Results Regarding the Possible Underlyuing Mecanisms Driving the Neutrinoless Double Beta Decay. *Front. Phys.* **2021**, *9*, 666591. [CrossRef]
16. Mirea, M.; Pahomi, T.; Stoica, S. Values of the phase Space Factors Involved in Double Beta Decay. *Rom. Rep. Phys.* **2015**, *67*, 035503.
17. Ajimura, S. et al. [CANDLES Collaboration]. Low background measurement in CANDLES-III for studying the neutrinoless double beta decay of ^{48}Ca. *Phys. Rev. D* **2021**, *103*, 092008. [CrossRef]
18. Agostini, M. et al. [GERDA Collaboration]. Final Results of GERDA on the Search for Neutrinoless Double-β Decay. *Phys. Rev. Lett.* **2020**, *125*, 252502. [CrossRef] [PubMed]
19. Azzolini, O.; Beeman, J.W.; Bellini, F.; Beretta, M.; Biassoni, M.; Brofferio, C.; Bucci, C.; Capelli, S.; Cardani, L.; Carniti, P.; et al. Final Result of CUPID-0 Phase-I in the Search for the ^{82}Se Neutrinoless Double-β Decay. *Phys. Rev. Lett.* **2019**, *123*, 032501. [CrossRef] [PubMed]
20. Argyriades, J. et al. [NEMO-3 Collaboration]. Measurement of the two neutrino double beta decay half-life of Zr-96 with the NEMO-3 detector. *Nucl. Phys. A* **2010**, *847*, 168. [CrossRef]

21. Armengaud, E.; Augier, C.; Barabash, A.S.; Bellini, F.; Benato, G.; Benoit, A.; Beretta, M.; Bergé, L.; Billard, J.; Borovlev, Y.A.; et al. New Limit for Neutrinoless Double-Beta Decay of ^{100}Mo from the CUPID-Mo Experiment. *Phys. Rev. Lett.* **2021**, *126*, 181802. [CrossRef]

22. Barabash, A.S.; Belli, P.; Bernabei, R.; Cappella, F.; Caracciolo, V.; Cerulli, R.; Chernyak, D.M.; Danevich, F.A.; d'Angelo, S.; Incicchitti, A.; et al. Final results of the Aurora experiment to study 2β decay of ^{116}Cd with enriched ^{116}CdWO$_4$ crystal scintillators. *Phys. Rev. D* **2018**, *98*, 092007. [CrossRef]

23. The CUORE Collaboration. Search for Majorana neutrinos exploiting millikelvin cryogenics with CUORE. *Nature* **2021**, *604*, 53.

24. Abe, S. et al. [KamLAND-Zen Collaboration]. Search for the Majorana Nature of Neutrinos in the Inverted Mass Ordering Region with KamLAND-Zen. *Phys. Rev. Lett.* **2023**, *130*, 051801. [CrossRef] [PubMed]

25. Arnold, R. et al. [NEMO-3 Collaboration]. Measurement of the $2\nu\beta\beta$ decay half-life of ^{150}Nd and a search for $0\nu\beta\beta$ decay processes with the full exposure from the NEMO-3 detector. *Phys. Rev. D* **2016**, *94*, 072003. [CrossRef]

26. Abgrall, N.; Abt, I.; Agostini, M.; Alexander, A.; Andreoiu, C.; Araujo, G.R.; Avignone, F.T., III; Bae, W.; Bakalyarov, A.; Balata, M.; et al. LEGEND-1000 Preconceptual Design Report. *arXiv* **2021**, arXiv:2107.11462v1.

27. Pavel, P. Povinecon behalf of the SuperNEMO collaboration, Background constrains of the SuperNEMO experiment for neutrinoless double beta-decay searches. *Nucl. Instr. Meth. A* **2017**, *845*, 398.

28. The CUPID Interest Group. CUPID pre-CDR. *arXiv* **2019**, arXiv:1907.09376.

29. The SNO+ Collaboration. The SNO+ experiment. *JINST* **2021**, *16*, P08059. [CrossRef]

30. nEXO Collaboration. NEXO: Neutrinoless double beta decay search beyond 10^{28} year half-life sensitivity. *J. Phys. G Nucl. Part. Phys.* **2022**, *49*, 015104. [CrossRef]

31. MAJORANA Collaboration. Final Result of the MAJORANA DEMONSTRATOR's Search for Neutrinoless Double-β Decay in ^{76}Ge. *Phys. Rev. Lett.* **2023**, *130*, 062501. [CrossRef]

32. Lee, M.H. et al. [AMoRE Collaboration]. AMoRE: A search for neutrinoless double-beta decay of 100Mo using low-temperature molybdenum-containing crystal detectors. *J. Instrum.* **2020**, *15*, C08010. [CrossRef]

33. Shirai, J. et al. [KamLAND-Zen Collaboration]. Results and future plans for the KamLAND-Zen experiment. *J. Phys. Conf. Ser.* **2017**, *888*, 012031. [CrossRef]

34. Anton, G. et al. [EXO-200 Collaboration]. Search for Neutrinoless Double-β Decay with the Complete EXO-200 Dataset. *Phys. Rev. Lett.* **2019**, *123*, 161802. [CrossRef] [PubMed]

35. Adams, C. et al. [NEXT Collaboration]. Sensitivity of a tonne-scale NEXT detector for neutrinoless double beta decay searches. *J. High Energy Phys.* **2021**, *8*, 164.

36. Chen, X.; Fu, C.; Galan, J.; Giboni, K.; Giuliani, F.; Gu, L.; Han, K.; Ji, X.; Lin, H.; Liu, J.; et al. PandaX-III: Searching for neutrinoless double beta decay with high pressure 136Xe gas time projection chambers. *Sci. China Phys. Mech. Astron.* **2017**, *60*, 061011. [CrossRef]

37. LUX-ZEPLIN (LZ) Collaboration. Projected sensitivity of the LUX-ZEPLIN experiment to the $0\nu\beta\beta$ decay of ^{136}Xe. *Phys. Rev. C* **2020**, *102*, 014602. [CrossRef]

38. Agostini, F.; Maouloud, S.E.; Althueser, L.; Amaro, F.; Antunovic, B.; Aprile, E.; Baudis, L.; Baur, D.; Biondi, Y.; Bismark, A.; et al. Sensitivity of the DARWIN observatory to the neutrinoless double beta decay of ^{136}Xe. *Eur. Phys. J. C* **2020**, *80*, 808. [CrossRef]

39. Ejiri, H.; Fushimi, K.; Hayashi, K.; Kishimoto, T.; Kudomi, N.; Kume, K.; Kuramoto, H.; Matsuoka, K.; Ohsumi, H.; Takahisa, K.; et al. Limits on the Majorana neutrino mass and right-handed weak currents by neutrinoless double b decay of ^{100}Mo. *Phys. Rev. C* **2001**, *63*, 065501. [CrossRef]

40. Ejiri, H.; Engel, J.; Hazama, R.; Krastev, P.; Kudomi, N.; Robertson, R.G. Spectroscopy of Double-Beta and Inverse-Beta Decays from ^{100}Mo for Neutrinos. *Phys. Rev. Lett.* **2000**, *85*, 2917. [CrossRef]

41. Ejiri, H.; Doe, P.; Elliott, S.R.; Engel, J.; Finger, M.; Finger, M.; Fushimi, K.; Gehman, V.; Greenfield, M.; Hazama, R.; et al. MOON for neutrino-less double beta decays. *Eur. Phys. J. Spec. Top.* **2008**, *162*, 239–250. [CrossRef]

42. Arnold, R.; Augier, C.; Bakalyarov, A.M.; Baker, J.; Barabash, A.; Bernaudin, P.; Bouchel, M.; Brudanin, V.; Caffrey, A.J.; Cailleret, J.; et al. Technical design and performance of the NEMO 3 detector. *Nucl. Instr. Methods A* **2005**, *536*, 79–122. [CrossRef]

43. Arnold, R.; Augier, C.; Baker, J.; Barabash, A.S.; Basharina-Freshville, A.; Bongrand, M.; Brudanin, V.; Caffrey, A.J.; Cebrián, S.; Chapon, A.; et al. Probing new physics models of neutrinoless double beta decay with SuperNEMO. *Eur. Phys. J. C* **2010**, *70*, 9270943. [CrossRef]

44. Suhonen, J. Impact of the quenching of g_A on the sensitivity of $0\nu\beta\beta$ experiments. *Phys. Rev. C* **2017**, *96*, 05501. [CrossRef]

45. Gysbers, P.; Hagen, G.; Holt, J.D.; Jansen, G.R.; Morris, T.D.; Navratil, P.; Papenbrock, T.; Quaglioni, S.; Schwenk, A.; Stroberg, S.R.; et al. Discrepancy between experimental and theoretical β decay rates resolved from first principles. *Nat. Phys.* **2018**, *15*, 428–431. [CrossRef]

46. Perez, E.A.C.; Menéndez, J.; Schwenk, A. Gamow-teller and doubleβ decays of heavy nuclei with an effective theory. *Phys. Rev.* **2018**, *98*, 045501.

47. Coraggio, L.; Angelis, L.D.; Fukui, T.; Gargano, A.; Itaco, N.; Nowacki, F. Renormalization of the Gamow-Teller operator within the realistic shell model. *Phys. Rev.* **2019**, *100*, 014316. [CrossRef]

48. Menéndez, J.; Gazit, D.; Schwenk, A. Chiral Two-Body Currents in Nuclei: Gamow-Teller Transitions and Neutrinoless Double-Beta Decay *Phys. Rev. Lett.* **2011**, *107*, 062501. [CrossRef] [PubMed]

49. Cappuzzello, F.; Lenske, H.; Cavallaro, M.; Agodi, C.; Auerbach, N.; Bellone, J. I.; Bijker, R.; Burrello, S.; Calabrese, S.; Carbone, D.; et al. Shedding light on nuclear aspects of neutrinoless double beta decay by heavy-ion double charge exchange reactions. *Prog. Part. Nucl. Phys.* **2023**, *128*, 103999. [CrossRef]

50. Ejiri, H.; Jokiniemi, L.; Suhonen, J. Nuclear matrix elements for neutrinoless $\beta\beta$-decays and spin dipole giant resonances. *Phys. Rev. C* **2022**, *105*, L022501. [CrossRef]